Molecular hierarchical release using hydrogenated graphene origami under electric field

Shuai Luo[1], A.S. Ademiloye[2], Zhengtian Wu[3], Yang Zhang[1,4,*]

[1]*School of Science, Nanjing University of Science and Technology, Nanjing, 210094, China*

[2]*Zienkiewicz Centre for Computational Engineering, College of Engineering, Swansea University Bay Campus, Swansea, SA1 8EN, UK*

[3]*School of Electronic and Information Engineering, Suzhou University of Science and Technology, Suzhou, 215009, China*

[4]*Department of Architecture and Civil Engineering, City University of Hong Kong, Kowloon, Hong Kong, China*

Abstract

In recent years, drug delivery has progressively become one of the main research areas in the field of biomedicine. However, the graded drug release remains a serious challenge at the nano-scales. Herein, we successfully simulated the graded release of C_{60} and C_{180} from the graphene box inspired by the origami technique under the control of an external electric field via molecular dynamics (MD) simulations. Our results provide a feasible scheme for hierarchical drug delivery at the nano-scales. The graphene origami was generated through the folding of graphene guided by its creases which were created by combining carbon atoms with hydrogen atoms and transforming sp^2 to sp^3 bonds at the combination line. We can construct complex graphene origami by designing reasonable hydrogen atoms distribution on graphene. This provides a simple and practicable program for designing complex graphene-based nanodevices for drug delivery.

Keywords: Graphene, Origami, Electric field, Self-folding, Drug delivery, MD simulation

* Corresponding author.
E-mail address: hfutzy@njust.edu.cn (Yang Zhang).

1. Introduction

Graphene is a two-dimensional carbon nanomaterial with hexagonal honeycomb lattice composed of carbon atoms with sp^2 hybrid orbitals [1]. Graphene has excellent optical, electrical and mechanical properties with important applications in various fields in science and engineering such as micro- and nano-fabrication [2, 3], energy harvesting [4, 5], biomedical applications [6, 7] and impact protection [8, 9], and it is considered as a revolutionary material for the future [10]. Graphene has a large surface-to-volume ratio, which makes it highly flexible in morphology, and because of the chemical diversity of carbon atoms, it has produced many structural derivatives through chemical modification methods, and these derived structures have novel functions [11-16]. For example, double-side hydrogenated graphene [17-20], graphene with single-sided hydrogenation [21, 22], fluorographene [23] and graphene-oxide [24, 25]. However, it has been reported in previous experimental studies that such modification of graphene changes its physical properties [25].

Recently, with the increasing application of graphene, it was discovered that chemically functionalized single-layer graphene can be folded into diverse and interesting nanostructures by rotating along the modification line [26, 27]. This interesting phenomenon shows strong similarity to origami, which is a technique that rotates paper along creases, transforming two-dimensional structures into complex three-dimensional structures. Based on the specific phenomenon and origami, the concept of graphene origami was introduced. Graphene origami can lead to various graphene-based structures that have a wide range of applications, such as drug delivery [28], supercapacitors [29], and hydrogen storage [30].

It is well-known that the creases play a pivotal role in the origami structure. The distribution of creases will induce the folding of the 3D structure and strengthen the stability of the structure. Inspired by origami technology, graphene nanobelts (GNRs) can be folded and extruded by forming sp3 bonds on graphene to generate creases. Guo et al. [31] showed that sp^2 bonds can be converted into sp^3 bonds in graphite and multi-walled carbon nanotubes (MWCNTs) under high pressure. Martins et al. [32] reported that the bilayer graphene will form diamondene with interlayer sp^3-bonding under high pressure. Hence, the transition from sp^2 to sp^3 can be achieved by employing high pressure on the graphene. However, the precise formation of sp^3 bonds by employing high pressure is still a challenge.

In the hydrogenated graphene, the hydrogen atoms change the atomic bond from sp^2 to sp^3, which causes a local deformation of graphene structure [12, 18, 19, 30, 33-37]. Recently,

unilateral hydrogenation of pristine graphene has been studied both theoretically and experimentally, and significant progress has been made in the precise hydrogenation of graphene [38]. For example, studies have demonstrated that hybrid superlattices made from functionalized hydrogenation can be fabricated in a controlled manner at both macro and micro scales [39]. Graphene can enhance the adsorption of hydrogen atoms when it bends locally [40, 41]. It has also been shown that graphene sheets can closely adhere to the sharp features of the substrate, resulting in local curvature of graphene [42, 43]. These indicate the feasibility of fabricating creases on graphene by precise hydrogenation.

Zhu et al. [30] employed hydrogen-functionalized graphene nanocages to control the simple uptake and release of nanoparticles, as well as the ultra-high density hydrogen storage. Reddy et al. [33] used hydrogenation to control the structure of graphene, thus creating complex graphene origami structures. It provides the possibility of graphene origami technology application in three-dimensional nanocircuits, flexible electronics, and so on.

Despite the hydrogenated graphene origami technology has been studied in many fields, there are few studies on the hierarchical release of nanoparticles from hydrogenated graphene nanobox under external electric field. Petri et al. [44] studied the biological effects of human exposure to electrostatic fields. Dawson et al. [45] reports that electric fields can be generated in the human due to electrostatic discharges. In particular, electric field-responsive nanoparticles and electric fields have attractive application potential in physical, chemical, biological mechanisms and therapeutics, and they has been widely studied as reported [46].

In this paper, molecular dynamics (MD) simulations are used to study the folding behavior of graphene monolayer with different hydrogenation modes under an external electric field. Firstly, the structure change modes of monolayer graphene corresponding to different hydrogenation modes are investigated. Following this, a three-dimensional graphene nanobox model was established. Then, the absorption and release of fullerene C_{60} were controlled by applying an external electric field. Finally, the hierarchical release of fullerenes C_{60} and C_{180} from the graphene nanobox was simulated by adjusting the electric field intensity. Our simulation results demonstrate that the hydrogenated graphene origami can be precisely controlled by the external electric field.

2. Methods

In this study, all the simulations are achieved with the Large-scale Atomic/Molecular Massively Parallel Simulator (LAMMPS) package, and visualization of atoms is accomplished by

visualizing molecular dynamics (VMD). We employed the Adaptive Intermolecular Reactive Empirical Bond Order (AIREBO) potential function [47] and Reactive Force Field (ReaxFF) potential [48], which are among the most widely used for reactive MD studies of carbon systems. In this research work, since there is no large hydrocarbon system, we disabled the torsional barrier in AIREBO, and only enabled the reactive empirical bond-order potential (REBO) potential and the Lennard-Jones (LJ) potential to describe the intra- and intermolecular interactions, respectively. In the simulation presented in section 3.1 and section 3.2, AIREBO potential is employed to describe C-C and C-H bonds in the graphene, as well as the non-bonded C-C and C-H interactions. To better show the effect of the external electric field, in the simulations presented in section 3.3 (except Fig. 6, which shows the charge distribution in the graphene nanobox) and section 3.4, the LJ potential in the AIREBO potential is modified to describe the non-bonded interactions while the REBO potential remains unchanged. The modified LJ potential (E) is given by formula:

$$E = 4\lambda\varepsilon\left[\left(\frac{\sigma}{\gamma}\right)^{12} - \left(\frac{\sigma}{\gamma}\right)^{6}\right] \quad (1)$$

where ε (= 0.00284 eV) is Lenard-Jones potential's depth and σ (= 0.34 nm) is the distance at which Lennard-Jones potential equals zero and λ represents the influence factor of the external electric field effect (when there is no external electric field, λ = 1, and when there is an external electric field, λ = 0.1) [30].

Since ReaxFF potentials can account for polarization effects by using geometrically correlated charge calculation schemes, the charge distribution in the simulation results shown in Fig. 6 were computed using the *reax/c* style in LAMMPS [48]. The initial temperature is set at 300 K.

The MD simulations in Figs. 1-3, and 7-11 were performed in the NVT ensemble. The initial temperature of these simulations is set at 300K, and the temperature is controlled by Nose-Hoover thermostat at 300K. The simulation results presented in Fig. 4 helps to demonstrate that the hydrogenated graphene nanobox is intrinsically energetically favorable. Prior to executing our MD simulations, we use the conjugate gradient algorithm and the steepest descent algorithm to minimize the energy until the relative error $\phi = \left[(E_n - E_{n-1}) / E_n\right] \leq 10^{-10}$, which is static simulation without kinetic energy in the system. However, the minimum iteration method may lead to the local minimum energy rather than global minimum energy. We can conduct the subsequent MD simulation in NVE ensemble to gain the global minimum potential energy by

running the dynamics with small or limited time steps [49]. In the NVE ensemble simulation, the maximum moving distance of the confined atom within a timestep is 0.1 Å and the initial temperature is set at 0 K. The time step is set to 0.5 femtoseconds (fs) in all simulations.

3. Simulation results and discussion

Carbon atoms on graphene form sp^3 C-H bonds after contacting hydrogen atoms, while chemically adsorbed hydrogen atoms repel other neighboring carbon atoms, which causes these neighboring carbon atoms to start away from hydrogen atoms, breaking the original planar structure and forming local bending. The local bending will vary depending on the location and density of hydrogen atoms adsorbed on graphene. If hydrogenation is performed on both sides of graphene, the resulting graphene will remain almost flat state, which is independent of the density of hydrogen atoms chemisorbed. However, if only one side of graphene is hydrogenated, the local bending will accumulate as the density of chemically adsorbed hydrogen atoms increases. For example, if hydrogen atoms are introduced linearly along one side of graphene, the local bending of graphene will form a folding angle when the structure reaches equilibrium, and the degree of this folding angle will gradually decrease as the number of rows of hydrogen atoms increases. This provides a possible scheme for precise and stable control of graphene folding. Based on these findings, we used LAMMPS to conduct a systematic MD simulation of the graded release of C_{60} and C_{180} fullerenes from graphene which is folded and unfolded by controlling the electric field.

3.1. Simulation of hydrogenation of monolayer graphene

Firstly, as shown in Fig. 1, we investigate how the hydrogen atom density affects the folding angle of monolayer graphene. Graphene is generally divided into zigzag graphene and armchair graphene. For these two types, the influence of one-line hydrogen atoms, two-line hydrogen atoms, and three-line hydrogen atoms on the folding angle of graphene is studied, and the simulation results are depicted in Fig. 2. With the increase of hydrogen line number on graphene, the folding angle at equilibrium decreases gradually. Under the same hydrogen line number, the folding angle of zigzag graphene is lower than that of armchair graphene. Especially, under two-line hydrogen atoms of zigzag graphene and three-line hydrogen atoms of armchair graphene, the equilibrium folding angles are close to 90 degrees.

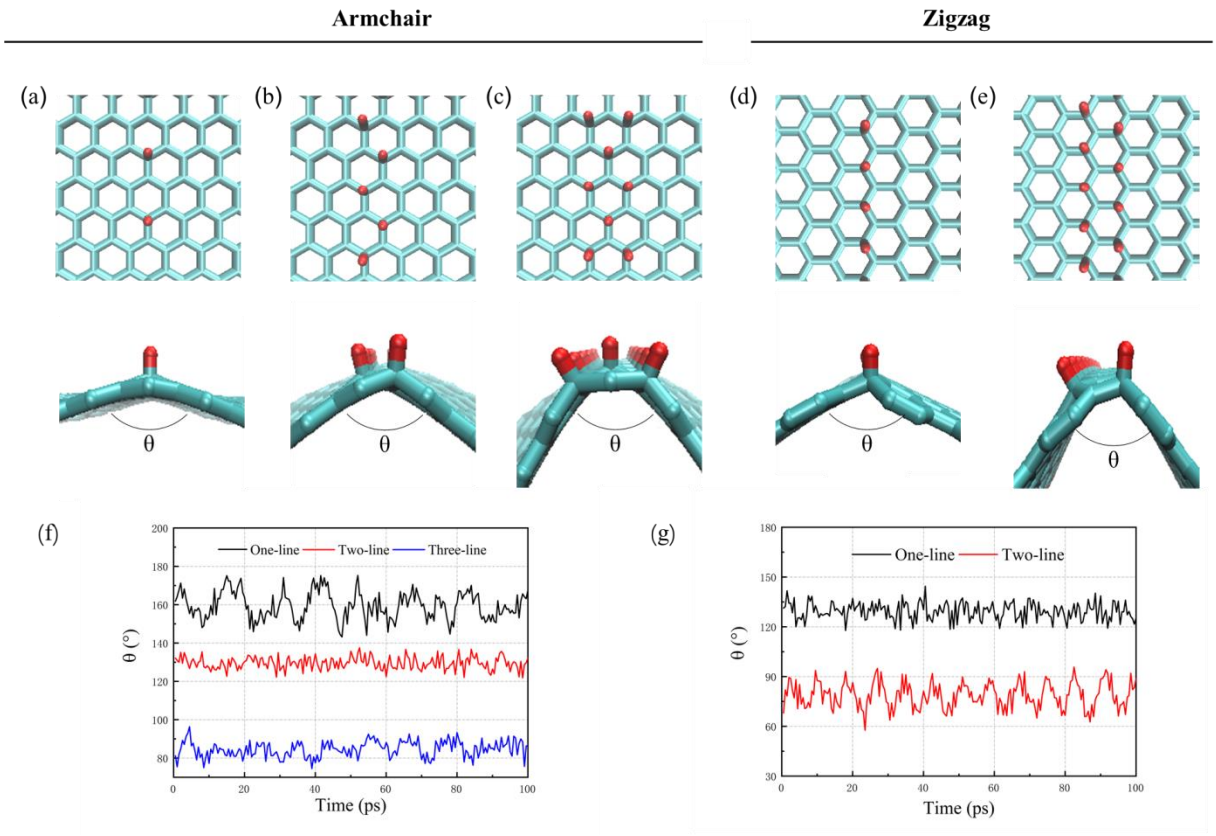

Fig. 1. Illustration of single-sided hydrogenated graphene. (a) One-line, (b) two-line, and (c) three-line hydrogenation along armchair direction of graphene. (d) One-line and (e) two-line hydrogenation along zigzag direction of graphene. (f) The variation of the folding angle of the armchair graphene at 300 K. (g) The variation of the folding angle of the zigzag graphene at 300 K.

The simulation results presented in Fig. 1 were obtained by introducing single-crease hydrogenation modes on graphene, and these simulation results are consistent with previous results [33]. If multiple hydrogenated creases are introduced into single graphene, to examine whether these creases affect each other, we simulated multiple-crease hydrogenation modes on graphene. Firstly, monolayer graphene on which the same creases are introduced at different positions is simulated. As illustrated in Fig. 2(a), two-line hydrogenation is introduced simultaneously on both sides of single-layer zigzag graphene, and then the energy relaxation is performed by MD simulation. The energy relaxation is done in the NVT ensemble and the temperature is controlled by Nose-Hoover thermostat at 300 K. The simulated folding angles are close to 90°.

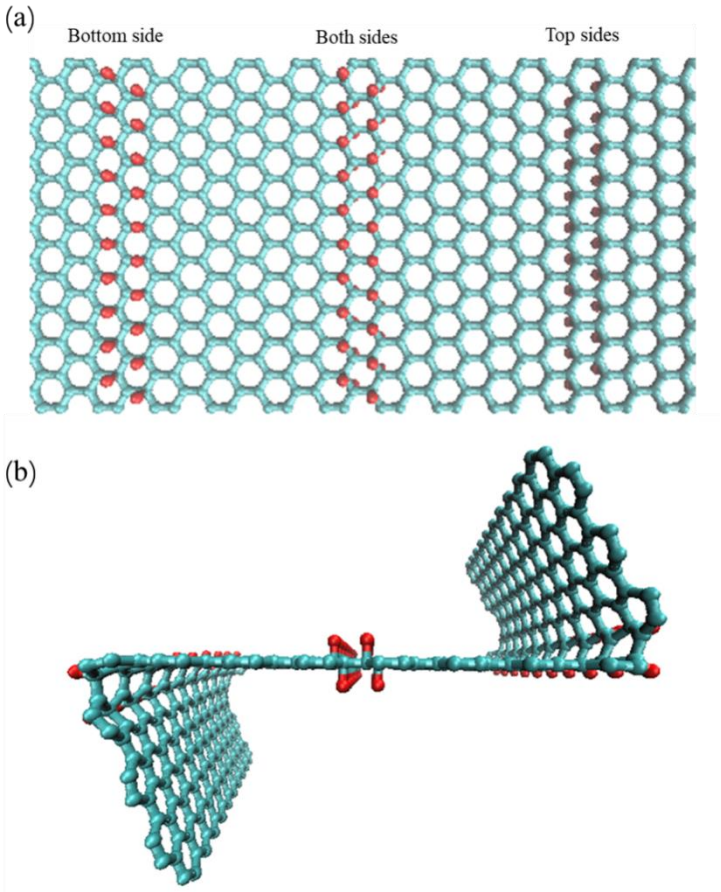

Fig. 2. (a) Top view of single-layer zigzag graphene with two-line hydrogenation. (b) Side view of the single-layer zigzag graphene after energy relaxation.

Then, the case that different creases are introduced at different positions on monolayer graphene is simulated. As shown in Fig. 3, we introduce two-line hydrogen atoms of zigzag graphene and three-line hydrogen atoms of armchair graphene simultaneously on the sheared cross-shaped graphene. The simulated folding angles are also close to 90°. These results are the same as those of the previous simulation in Fig. 1. It can be observed from Fig. 2(b) and Fig. 3(b) that multiple-crease hydrogenation gives the same results with those in single-crease hydrogenation; that is, creases are independent of each other.

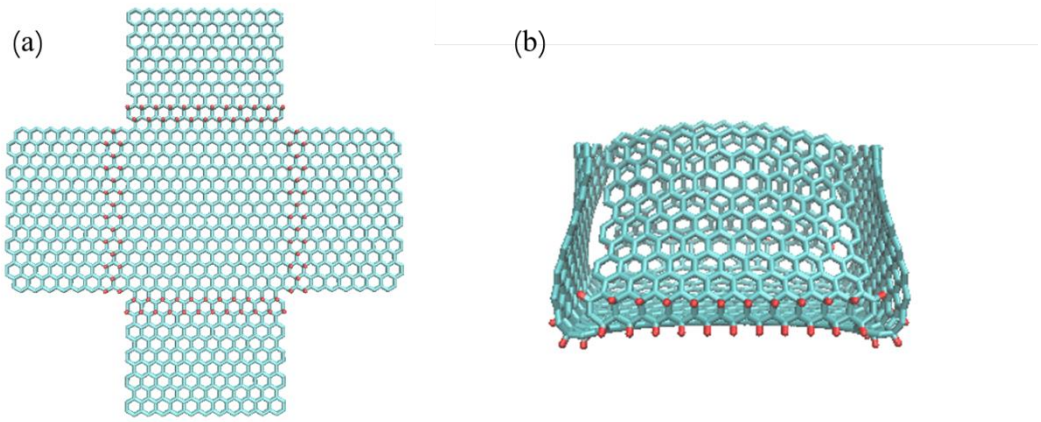

Fig. 3. (a) Top view of graphene with multiple hydrogenation creases. (b) Folding behavior of hydrogenated graphene sheet at 300 K

3.2. Hydrogenated graphene hexahedral nanobox

Based on the above simulations, we explore the idea of simulating a hexahedral nano box which can deliver drug particles. The designed hexahedron nanobox model based on a single-layer double-cross shaped graphene is exhibited in Fig. 4 (a), in which the length L = 12.8 nm and width W = 7.1 nm. In the present structure, we introduce two-line and three-line hydrogen atoms at the corresponding crease simultaneously, making the folding angles of these positions close to 90 degrees. The whole double-cross graphene model is divided into nine regions. On the six outer regions of the graphene sheet, hydrogen atoms are saturated on the edge because there are two purposes. On the one hand, it is to prevent the formation of unnecessary bonds due to unsaturation of carbon atoms at the edges during self-assembly, and on the other hand, to make the edges of the six outer regions have hydrogen lines, paving the way for the subsequent introduction of external electric field simulation.

During the energy minimization calculations, which is static simulation without kinetic energy, the folding angles of outer region creases of double-cross graphene gradually approach 90 degrees. In the following MD simulation, the double-cross graphene closes, and its potential energy reaches the lowest point. However, the structure does not reach a stable state at this time, and the hexahedral nanobox structure is not regular. After a period of relaxation time, the system reaches equilibrium due to geometrical constraints and interlayer van der Waals force (vdW) interaction, and double-cross graphene folds into hexahedral nanobox. The potential energy variation corresponding to the four cases in Fig. 4 is illustrated in Fig. 5.

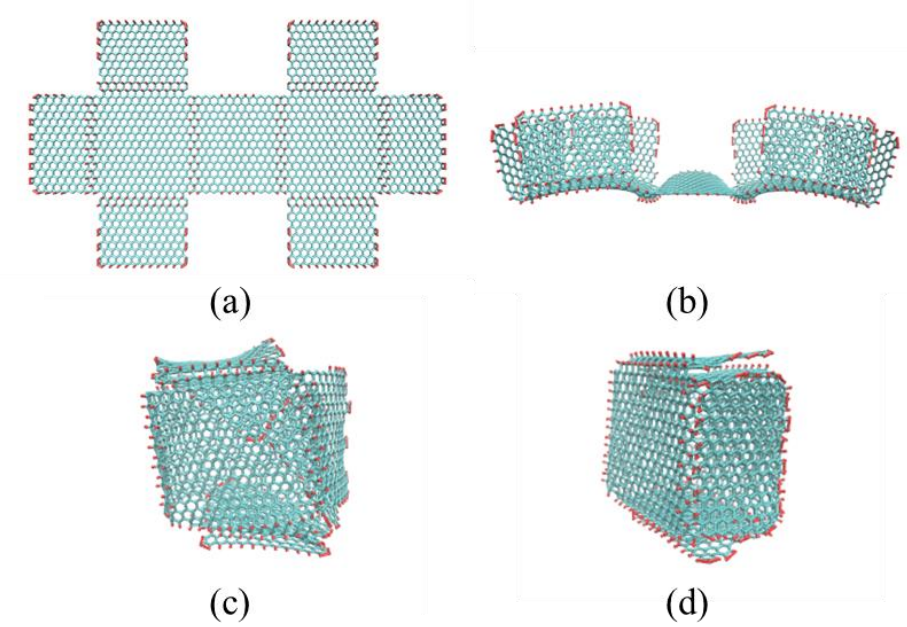

Fig. 4. (a) Top view of double-cross hydrogenated graphene. (b-d) Structure change of double-crosses hydrogenated graphene.

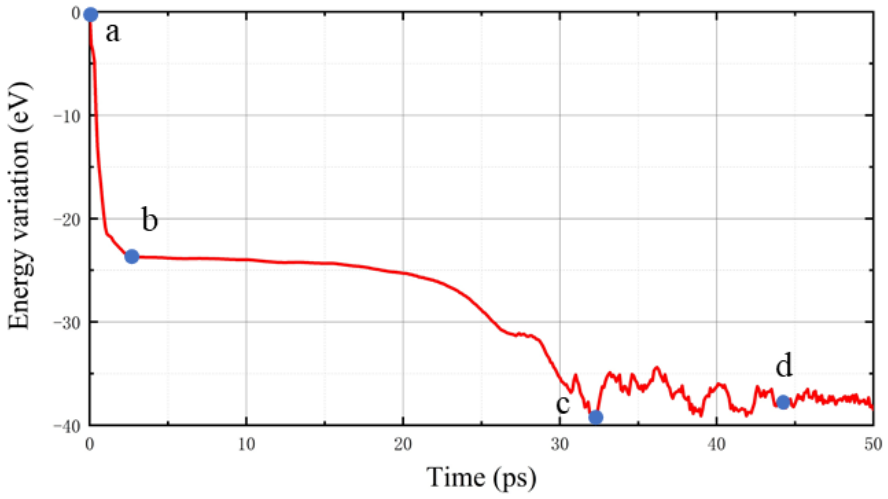

Fig. 5. Potential energy variation of hydrogenated graphene nanobox without external electric field.

In the simulation of hydrogenated graphene hexahedral nanobox, the interlayer vdW interaction is the pivotal factor to stabilize the graphene hydride nanostructure. If we can control this interaction, it will provide a feasible solution for controlling the morphology of graphene nanobox (for example, hexahedron nanobox open and close).

3.3. Simulation of graphene nanobox structure controlled by external electric field

The first-principles calculations reveal the dependence of effective boundary electrical constants in graphene structures on applied electric fields. Graphene nanostructures have various intrinsic dipole moments due to the uneven distribution of charges throughout the structure because of chemical modification and subsequent structural changes. When there is no external electric field, the orientation of the intrinsic dipole moment of the molecule in the medium is irregular due to thermal motion, so the vector sum of the dipole moment is zero, and the medium does not have macroscopic polarization strength. Under the action of an external electric field, first, the electric field causes the polarization of atoms in graphene, and second, the dipole moments in the molecules will be arranged along the direction of the electric field, resulting in non-zero dipole moments. Therefore, the structural polarization induced by the applied electric field can change the interlayer interaction.

Due to hydrogenation causing hexahedron nanostructures global polarization effect, therefore we use ReaxFF potential to calculate charge distribution of the structure. As illustrated in Fig. 6, because of the electronegativity difference between hydrogen and carbon atoms, hydrogen atoms have the highest positive charge while the carbon atoms near to hydrogen atoms have the highest negative charge. The other carbon atoms have a quite low negative charge. When an external electric field is applied, these positively charged hydrogen atoms and negatively charged carbon atoms will experience local electrostatic forces in the opposite direction. Therefore, the folded edges in the nanobox experience local electrostatic torque. The distribution of positive and negative charges in the nanobox is plotted in Fig. 6 (b). The middle part of each surface of the nanobox is negatively charged, while the edge is positively charged. This polarization mode results in the formation of large-scale molecular dipoles in the nanobox, which can generate torque under the external electric field causing the spreading of graphene nanobox. To demonstrate the effect of the external electric field on the structure change of the graphene nanobox, MD simulations were performed by imposing different electric field strength in a specified direction.

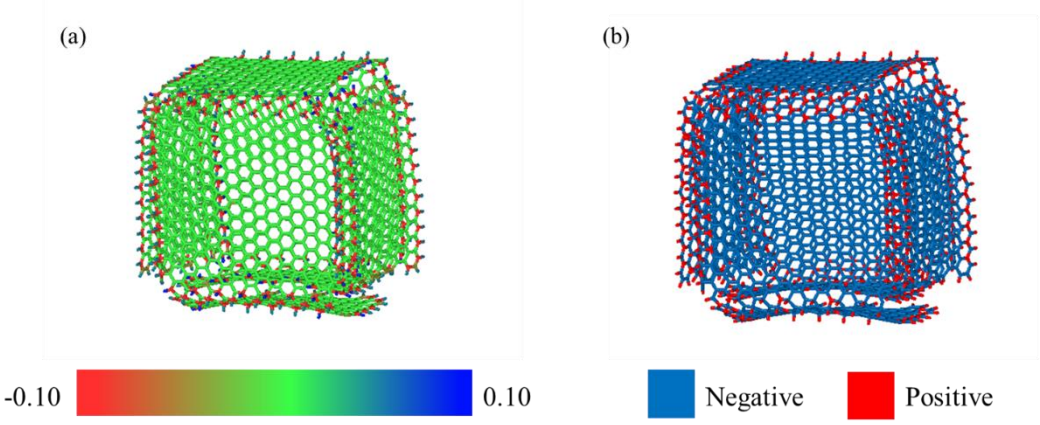

Fig. 6. (a) Hydrogenation and folding induced non-uniform charge distribution in the graphene nanobox. (b) Distribution of positive and negative charges in the graphene nanobox.

Following the above enlightenment, we demonstrate that the opening and closing of hexahedral nanocages made of graphene hydride can be controlled by adjusting the interlayer interaction through the external electric field from a fixed direction.

Fig. 7 shows that hydrogenated graphene under normal interlayer vdW interaction spontaneously forms a closed nanobox structure. Firstly, a weaker external electric field is imposed (electric field strength E = 0.1 V/ Å) and the graphene structure hardly change. However, when the external electric field strength increases to E = 0.16 V/ Å, the nanobox structure became unstable and the closed nanobox gradually opens. Conversely, after the removal of the external electric field, the opened graphene nanostructure gradually closes. Through the switch of the external electric field, we can obtain an opened or closed graphene nanobox, and the entire process is reversible.

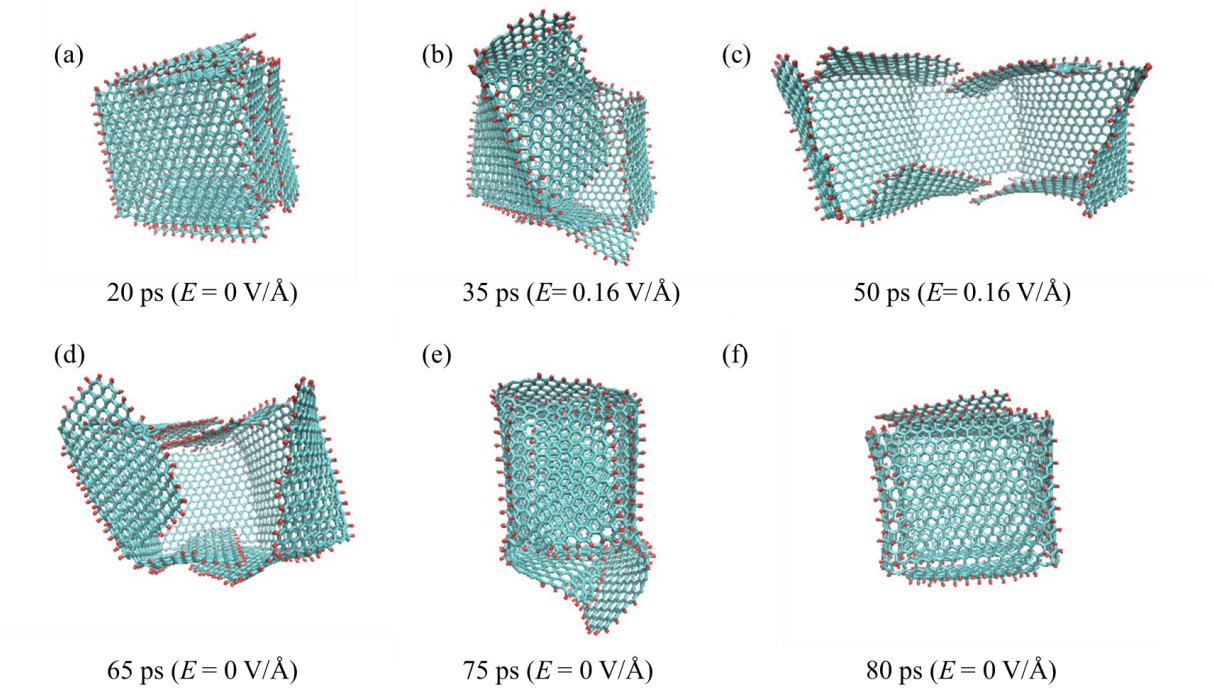

Fig. 7. (a) Stable hydrogenated graphene nanobox at 300K. (b-c) The opening process of hydrogenated graphene nanobox under external electric field. (d-f) The closing process of hydrogenated graphene nanobox after removing the external electric field.

In the previous simulation, when the external electric field is applied or removed, the energy of the system will change. As shown in Fig. 8, the nanobox is closed initially and the system energy fluctuates steadily in a small range. When the external electric field (E = 0.16 V/ Å) is applied during 50-90 ps and 150-190 ps, the nanobox gradually opens, and the energy of the system increases significantly, then it stabilizes and fluctuates in a small range. When the external electric field is removed, the nanobox starts to close and the system energy is reduced to the value that fluctuates steadily when no electric field is applied.

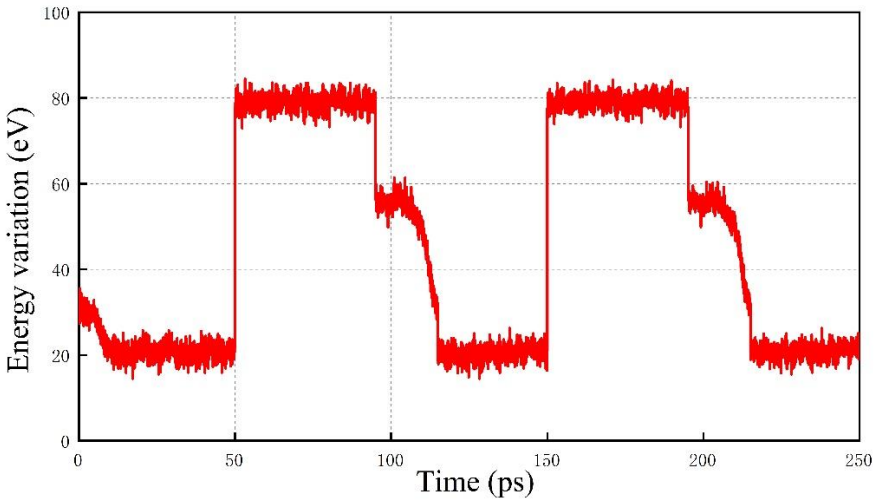

Fig. 8. Energy variation of hydrogenated graphene nanobox with or without an external electric field. During 0-50 ps, 90-150 ps and 190-250 ps, nanobox closes without external electric field; during 50-90 ps and 150-190 ps, nanobox opens with external electric field

Our simulation results indicate that when imposing a weaker external electric field, the electrostatic forces or moments generated by the external electric field is insufficient to overcome interlayer interactions. However, when the external electric field strength is large enough, there is enough electrostatic force or moment imposed on the hexahedral nanobox to overcome the interlayer interaction causing the nanobox opening.

To explore the effect of the relative orientation of the cage and the electric field, we performed a set of simulations in which an electric field with a strength of 0.2 V/Ang is applied from the 6 sides of the graphene box. As illustrated in Fig. 9 (a), these arrows represent the direction of the electric field. As shown in Fig. 9 (b), the results obtained show that the graphene box can be opened and closed normally under various conditions, which is due to the polarization effect of hexahedral structure and the application of strong electric field (0.2 V/Ang).

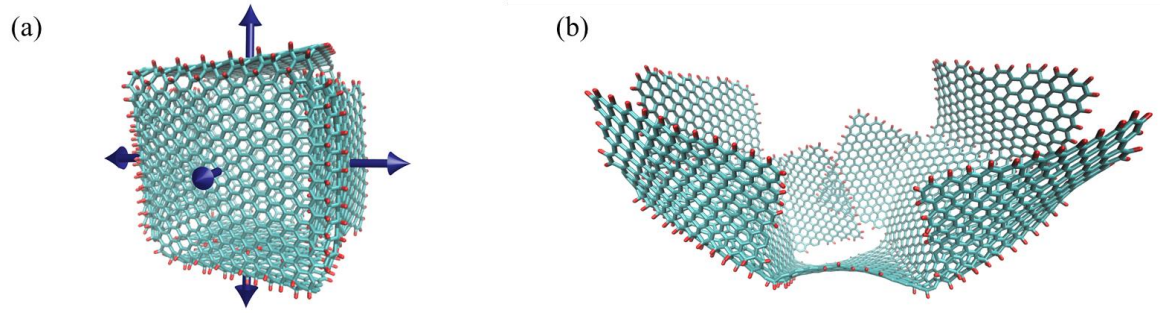

Fig. 9. (a) The electric field is applied from the 6 sides of the graphene box. (b) The unfolding of the graphene box with external electric field.

The controllable graphene nanobox are of practical significance for effective drug delivery. For example, as displayed in Fig. 8, graphene nanobox can serve as nanocontainers for molecular transfer. As shown in Fig. 10 (a-d), initially, hydrogenated graphene hexahedral nanobox is placed together with C_{60} molecules. Because of the thermal effect, C_{60} moves continuously in space. When an external electric field is imposed, the nanobox gradually opens. When the nanobox opens to a certain extent, the external electric field is switched off, and the hydrogenated graphene nanobox closes gradually. During this period, some C_{60} molecules enter the nano box driven by thermal fluctuation. It can be observed from Fig. 10 (e-h) that when the hydrogenated graphene nanobox is completely closed, there is a C_{60} molecule in the nanobox. Then, an external electric field is imposed again, the hydrogenated graphene nanobox gradually opens. As the nano box opens, the C_{60} molecule in the nanobox keeps moving and finally leave the nanobox. Finally, after removing the external electric field, the hydrogenated graphene box closes.

The above investigation is to simulate the hydrogenated graphene nanobox used as a nano container for single-molecule absorption and release. The absorption process of the hydrogenated graphene nanobox is shown in Fig. 10 (a-d) while Fig. 10 (e-h) shows the molecule release process. Our simulation results prove that the hydrogenated graphene nanobox has the potential as a nanocontainer for effective molecule transfer with practical applications in the field of drug delivery.

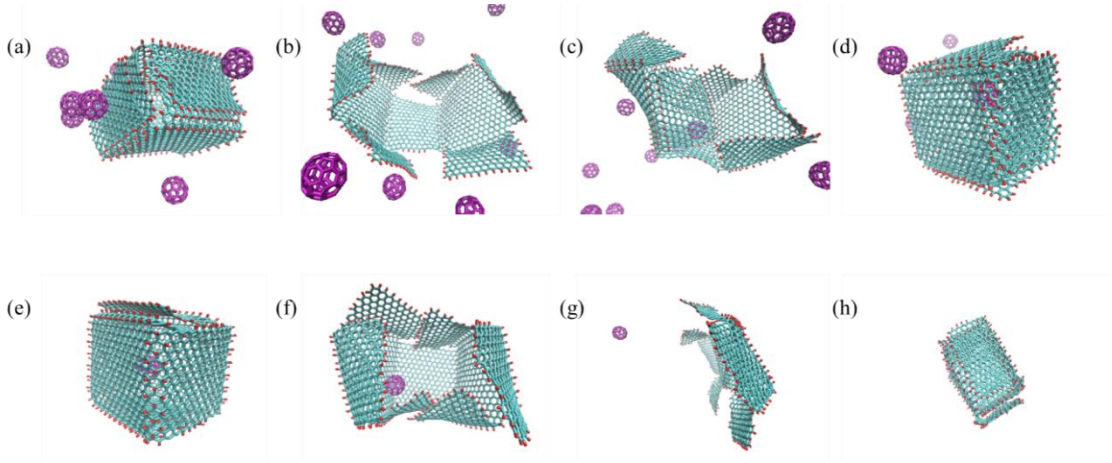

Fig. 10. (a-d) The process of capturing C_{60}. (e-h) The process of releasing C_{60} from hydrogenated graphene nanobox

3.4. Simulation of hierarchical release of graphene nanobox under electric field

Following the previous simulation, we again explore the hypothesis that the hydrogenated graphene nanobox can be used as a nano container for the graded release of molecules by controlling the external electric field. To confirm the validity of this hypothesis or idea, we perform further MD simulations and the obtained simulation results are presented in this section.

As illustrated in Fig. 11 (a), there are two kinds of molecules (C_{60} and C_{180}) in the hydrogenated graphene nanobox. When the external electric field (E = 0.15 V/ Å) is applied to the system, the hydrogenated graphene nanobox is slowly opened and finally, the hydrogenated graphene nanobox maintains a certain angle, as depicted in Fig. 11 (b). Fig. 11 (c) shows that C_{60} and C_{180} move continuously in the hydrogenated graphene nanobox due to thermal effect. However, the opening size of the hydrogenated graphene nanobox can only let C_{60} molecules rather than C_{180} molecules in and out. Therefore, C_{60} molecules moved out of the hydrogenated graphene nanobox while C_{180} remains in the nano box. Then, the external electric field is removed and the nano-box closes, leaving the C_{180} molecule in it. Afterward, a stronger electric field (E = 0.25 V/ Å) is applied and the box is completely opened, leaving both C_{60} and C_{180} molecules out of it. The simulation perfectly demonstrates that by controlling the intensity of the external electric field, the opening degree of the hydrogenated graphene nanobox can be

controlled. Therefore, it can be used to realize the hierarchical absorption and release of nanoparticles.

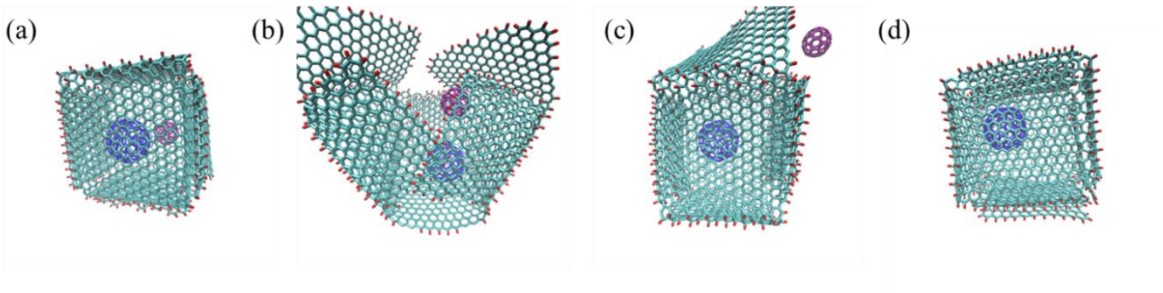

Fig. 11. (a-d) Selectively release of C_{60} from hydrogenated graphene nano box under external electric field.

4. Conclusion

In this work, the effect of the hydrogen atom as the crease of graphene origami and the effect of the exogenous electric field on the hydrogenated graphene nanobox were comprehensively studied using MD simulations. Various origami structures derived from graphene can be obtained by adjusting the distribution of creases. Our MD simulation results show that the opening and closure of hydrogenated graphene nanobox can be precisely controlled by adjusting the external electric field parameters. Finally, the graded release of C_{60} and C_{180} from the hydrogenated graphene nanobox was successfully simulated. Our simulation results show that the hydrogenated graphene nanobox can be used for molecular uptake, transport, and release at the nano-scale and it widens the potential application of graphene since different distribution of creases on graphene can be employed to derive different graphene nanostructures.

Acknowledgments

This work was supported in part by NSFC under Grant No. 11902159, the Hong Kong Scholars Program (Project No. XJ2019016) and Natural Science Foundation of Jiangsu Province under Grant No. BK20170820.

References

[1] A.K. Geim, K.S. Novoselov, The rise of graphene, Nature Materials 6(3) 183-191.
[2] J.H. Kim, Y. Choi, J. Kang, E. Choi, S.E. Choi, O. Kwon, D.W. Kim, Scalable fabrication of deoxygenated graphene oxide nanofiltration membrane by continuous slot-die coating, Journal of Membrane ence (2020).
[3] J. Chen, J. Meng, Y. Zhou, H. Wu, Y. Bie, Z. Liao, D. Yu, Layer-by-layer assembly of vertically conducting graphene devices, Nature Communications 4(1) (2013) 1921.
[4] A. Allahbakhsh, M. Arjmand, Graphene-based Phase Change Composites for Energy Harvesting and Storage: State of the Art and Future Prospects, Carbon (2019).
[5] H.J. Kim, S.Y. Lee, L.H. Sinh, C.S. Yeo, Y.R. Son, K.R. Cho, Y.K. Song, S. Ju, M.K. Shin, S.J. Park, Maximizing volumetric energy density of all-graphene-oxide-supercapacitors and their potential applications for energy harvest, Journal of Power Sources 346(APR.1) (2017) 113-119.
[6] A.P. Johnson, H.V. Gangadharappa, K. Pramod, Graphene nanoribbons: A promising nanomaterial for biomedical applications, J Control Release 325 (2020) 141-162.
[7] M.E. Foo, S.C.B. Gopinath, Feasibility of graphene in biomedical applications, Biomed Pharmacother 94 (2017) 354-361.
[8] Y. Qiu, Y. Zhang, A.S. Ademiloye, Z. Wu, Molecular dynamics simulations of single-layer and rotated double-layer graphene sheets under a high velocity impact by fullerene, Computational Materials Science 182 (2020).
[9] S. Vignesh, R. Surendran, T. Sekar, B. Rajeswari, Ballistic impact analysis of graphene nanosheets reinforced kevlar-29, Materials Today: Proceedings (2020).
[10] A.K.M.A. Iqbal, N. Sakib, A.K.M.P. Iqbal, D.M. Nuruzzaman, Graphene-based nanocomposites and their fabrication, mechanical properties and applications, Materialia 12 (2020).
[11] T. Li, Extrinsic morphology of graphene, Modelling & Simulation in Materials Science & Engineering 19(5) (2011) 599-605.
[12] D.C. Elias, R. Nair, T. Mohiuddin, S.V. Morozov, P. Blake, M.P. Halsall, A. Ferrari, D.W. Boukhvalov, M.I. Katsnelson, A.K. Geim, Control of Graphene's Properties by Reversible Hydrogenation: Evidence for Graphane, Science 323(5914) (2009) 610-613.
[13] M. Jafaryzadeh, C.D. Reddy, Y. Zhang, A chemical route to control molecular mobility on graphene, Physical Chemistry Chemical Physics 14(30) (2012) 10533-10539.
[14] J. Feng, W. Li, X. Qian, J. Qi, L. Qi, J. Li, Patterning of graphene, Nanoscale 4(16) (2012) 4883-4899.
[15] T. Kuilla, S. Bhadra, D. Yao, N.H. Kim, S. Bose, J.H. Lee, Recent advances in graphene based polymer composites, Progress in Polymer Science 35(11) (2010) 1350-1375.
[16] H. Shi, H. Pan, Y. Zhang, B.I. Yakobson, Electronic and Magnetic Properties of Graphene/Fluorographene Superlattices, Journal of Physical Chemistry C 116(34) (2012) 18278-18283.
[17] J.O. Sofo, A. Chaudhari, G.D. Barber, Graphane: A two-dimensional hydrocarbon, Physical Review B 75(15) (2007) 153401.
[18] S. Zhu, T. Li, Hydrogenation enabled scrolling of graphene, Journal of Physics D 46(7) (2013) 075301.
[19] A.A. Dzhurakhalov, F.M. Peeters, Structure and energetics of hydrogen chemisorbed on a single graphene layer to produce graphane, Carbon 49(10) (2011) 3258-3266.
[20] O.V. Pupysheva, A.A. Farajian, B.I. Yakobson, Fullerene Nanocage Capacity for Hydrogen Storage, Nano Letters 8(3) (2008) 767-774.
[21] X. Wang, G. Zhang, Z. Wang, L. Yang, X. Li, J. Jiang, Y. Luo, Metal-enhanced hydrogenation of graphene with atomic pattern, Carbon 143 (2019) 700-705.
[22] R. Balog, B. Jorgensen, L. Nilsson, M. Andersen, E. Rienks, M. Bianchi, M. Fanetti, E. Laegsgaard, A. Baraldi, S. Lizzit, Z. Sljivancanin, F. Besenbacher, B. Hammer, T.G. Pedersen, P. Hofmann, L. Hornekaer, Bandgap opening in graphene induced by patterned hydrogen adsorption, Nat Mater 9(4) (2010) 315-9.
[23] K. Worsley, P. Ramesh, S.K. Mandal, S. Niyogi, M.E. Itkis, R.C. Haddon, Soluble graphene derived from graphite fluoride, Chemical Physics Letters 445(1) (2007) 51-56.

[24] D.A. Dikin, S. Stankovich, E. Zimney, R.D. Piner, G. Dommett, G. Evmenenko, S.T. Nguyen, R.S. Ruoff, Preparation and characterization of graphene oxide paper, Nature 448(7152) (2007) 457-460.
[25] G. Eda, G. Fanchini, M. Chhowalla, Large-area ultrathin films of reduced graphene oxide as a transparent and flexible electronic material, Nature Nanotechnology 3(5) (2008) 270-274.
[26] Q.X. Pei, Y.W. Zhang, V.B. Shenoy, A molecular dynamics study of the mechanical properties of hydrogen functionalized graphene, Carbon 48(3) (2010) 898-904.
[27] K. Drogowska-Horná, V. Valeš, J. Plšek, M. Michlová, J. Vejpravová, M. Kalbáč, Large scale chemical functionalization of locally curved graphene with nanometer resolution, Carbon 164 (2020) 207-214.
[28] Y. Wang, C. Wang, Self-assembly of graphene sheets actuated by surface topological defects: Toward the fabrication of novel nanostructures and drug delivery devices, Applied Surface Science 505 (2020).
[29] C. Liu, Z. Yu, D. Neff, A. Zhamu, B.Z. Jang, Graphene-based supercapacitor with an ultrahigh energy density, Nano Lett 10(12) (2010) 4863-8.
[30] S. Zhu, T. Li, Hydrogenation-assisted graphene origami and its application in programmable molecular mass uptake, storage, and release, ACS Nano 8(3) (2014) 2864-2872.
[31] Wanlin, Guo, C., Z., Zhu, T., X., Yu, C., H., Formation ofsp3Bonding in Nanoindented Carbon Nanotubes and Graphite, Physical Review Letters (2004).
[32] L.G.P. Martins, M.J.S. Matos, A.R. Paschoal, P.T.C. Freire, N.F. Andrade, A.L. Aguiar, J. Kong, B.R.A. Neves, A.B. De Oliveira, M.S.C. Mazzoni, Raman evidence for pressure-induced formation of diamondene, Nature Communications 8(1) (2017) 96.
[33] C.D. Reddy, Y. Zhang, Structure manipulation of graphene by hydrogenation, Carbon 69 (2014) 86-91.
[34] R. Balog, B. Jorgensen, L. Nilsson, M. Andersen, E. Rienks, M. Bianchi, M. Fanetti, E. Laegsgaard, A. Baraldi, S. Lizzit, Bandgap opening in graphene induced by patterned hydrogen adsorption, Nature Materials 9(4) (2010) 315-319.
[35] L. Ci, Z.P. Xu, L. Wang, W. Gao, F. Ding, K.F. Kelly, B.I. Yakobson, P.M. Ajayan, Controlled nanocutting of graphene, Nano Research 1(2) (2008) 116-122.
[36] J.S. Burgess, B.R. Matis, J.T. Robinson, F.A. Bulat, F.K. Perkins, B.H. Houston, J.W. Baldwin, Tuning the electronic properties of graphene by hydrogenation in a plasma enhanced chemical vapor deposition reactor, Carbon 49(13) (2011) 4420-4426.
[37] O.C. Compton, S.W. Cranford, K.W. Putz, Z. An, L.C. Brinson, M.J. Buehler, S.T. Nguyen, Tuning the Mechanical Properties of Graphene Oxide Paper and Its Associated Polymer Nanocomposites by Controlling Cooperative Intersheet Hydrogen Bonding, ACS Nano 6(3) (2012) 2008-2019.
[38] D.C. Elias, R.R. Nair, T.M.G. Mohiuddin, S.V. Morozov, P. Blake, M.P. Halsall, A.C. Ferrari, D.W. Boukhvalov, M.I. Katsnelson, A.K. Geim, Control of graphene's properties by reversible hydrogenation, Physics 323(5914) (2008) 610-3.
[39] Z. Sun, C.L. Pint, D.C. Marcano, C. Zhang, J. Yao, G. Ruan, Z. Yan, Y. Zhu, R.H. Hauge, J.M. Tour, Towards hybrid superlattices in graphene, Nature Communications 2 (2011) 559-0.
[40] L.A. Chernozatonskii, P.B. Sorokin, Nanoengineering Structures on Graphene with Adsorbed Hydrogen "Lines", Journal of Physical Chemistry C 114(7) (2010) 3225-3229.
[41] P. Ruffieux, O. Grning, M. Bielmann, P. Mauron, P. Grning, Hydrogen adsorption on sp2-bonded carbon: Influence of the local curvature, Phys.rev.b 66(24) (2002) 126-130.
[42] S. Zhu, T. Li, Wrinkling Instability of Graphene on Substrate-Supported Nanoparticles, Journal of Applied Mechanics 81(6) 061008.
[43] C.H. Lui, L. Liu, K.F. Mak, G.W. Flynn, T.F. Heinz, Ultraflat graphene, Nature 462(nov.19) (2009) 339-341.
[44] A.K. Petri, K. Schmiedchen, D. Stunder, D. Dechent, T. Kraus, W.H. Bailey, S. Driessen, Biological effects of exposure to static electric fields in humans and vertebrates: a systematic review, Environmental Health 16(1) (2017) 41.
[45] T.W. Dawson, M.A. Stuchly, R. Kavet, Electric fields in the human body due to electrostatic discharges, IEEE Transactions on Biomedical Engineering 51(8) (2004) 1460-1468.

[46] J. Kolosnjaj-Tabi, L. Gibot, I. Fourquaux, M. Golzio, M.P. Rols, Electric field-responsive nanoparticles and electric fields: physical, chemical, biological mechanisms and therapeutic prospects, Advanced Drug Delivery Reviews 138 (2019) 56-67.
[47] S.J. Stuart, A.B. Tutein, J.A. Harrison, A reactive potential for hydrocarbons with intermolecular interactions, The Journal of Chemical Physics 112(14) (2000) 6472-6486.
[48] K. Chenoweth, A.C.T.V. Duin, W.A. Goddard, ReaxFF Reactive Force Field for Molecular Dynamics Simulations of Hydrocarbon Oxidation, The Journal of Physical Chemistry A 112(5) (2008) 1040-1053.
[49] S. Sihn, V. Varshney, A.K. Roy, B.L. Farmer, Modeling for predicting strength of carbon nanostructures, Carbon 95 (2015) 181-189.